Conference materials
UDC 621.373.826
DOI: https://doi.org/10.18721/JPM/161.328

1.55 μm optical-fiber transmitter based on vertical cavity surface emitting laser obtained by wafer fusion technology

Ya.N. Kovach [1] ✉, S.A. Blokhin [1], A.V. Babichev [2], M.A. Bobrov [1],
A.A. Blokhin [1], A.G. Gladyshev [3], I.I. Novikov [2],
L.Ya. Karachinsky [2], K.O. Voropaev [4], A.Yu. Egorov [3]

[1] Ioffe Institute, St. Petersburg, Russia;
[2] ITMO University, St. Petersburg, Russia;
[3] Connector Optics LLC, St. Petersburg, Russia;
[4] JSC OKB-Planeta, Veliky Novgorod, Russia
✉ yakovachyakov@gmail.com

Abstract. In this work, the static and dynamic characteristics of a 1.55 μm optical-fiber transmitter based on wafer-fused VCSEL were studied. The device demonstrated single-mode lasing with SMSR >30 dB over a wide range of currents, and the maximum optical output power at the fiber end more than 2.5 mW. The measured −3 dB modulation bandwidth exceeded 11 GHz, and the maximum bit rate achieved was 25 Gbps. Analysis of the lasing spectra under different amplitude modulations was carried out. Positive chirping (spectra broadening) and fiber chromatic dispersion were limiting factors for the data transmission over SMF-28 fiber.

Keywords: VCSEL, optical-fiber transmitter, chirping, wafer-fusion, data transmission

Funding: The authors from ITMO University were funded by Advanced Engineering Schools Federal Project for studies on the dynamic characteristics, and by the Ministry of Science and Higher Education of the Russian Federation for studies on the static characteristics (Project 2019-1442).

Citation: Kovach Ya.N., Blokhin S.A., Babichev A.V., Bobrov M.A., Blokhin A.A., Gladyshev A.G., Novikov I.I., Karachinsky L.Ya., Voropaev K.O., Egorov A.Yu., 1.55 μm optical-fiber transmitter based on vertical cavity surface emitting laser obtained by wafer fusion technology. St. Petersburg State Polytechnical University Journal. Physics and Mathematics. 16 (1.3) (2023) 163–169. DOI: https://doi.org/10.18721/JPM.161.328

Материалы конференции
УДК 621.373.826
DOI: https://doi.org/10.18721/JPM.161.328

Волоконно-оптический передатчик спектрального диапазона 1.55 мкм на основе вертикально-излучающего лазера, изготовленного с применением технологии спекания пластин

Я.Н. Ковач [1] ✉, С.А. Блохин [1], А.В. Бабичев [2], М.А. Бобров [1],
А.А. Блохин [1], А.Г. Гладышев [3], И.И. Новиков [2],
Л.Я. Карачинский [2], К.О. Воропаев [4], А.Ю. Егоров [3]

[1] Физико-технический институт им. А.Ф. Иоффе РАН, Санкт-Петербург, Россия;
[2] Университет ИТМО, Санкт-Петербург, Россия;
[3] ООО "Коннектор Оптикс", Санкт-Петербург, Россия;
[4] ОАО "ОКБ-Планета", г. Великий Новгород, Россия
✉ yakovachyakov@gmail.com

Аннотация. В работе были исследованы статические и динамические характеристики оптоволоконного передатчика на основе ВИЛ спектрального диапазона 1.55 мкм, полученного технологией спекания пластин. Прибор демонстрирует одномодовую генерацию с SMSR >30 дБ в широком диапазоне рабочих токов, а максимальная оптическая мощность на выходе волокна превышает 2.5 мВт. Измеренная эффективная частота модуляции превышает 11 ГГц, а максимальная достигнутая скорость передачи данных составила 25 Гбит/с. Был проведен анализ спектров излучения при различной амплитудной модуляции. Положительный чирпинг-эффект (уширение спектра) и хроматическая дисперсия волокна лимитируют дальность передачи данных.

Ключевые слова: ВИЛ, волоконно-оптический передатчик, чирпинг-эффект, спекание пластин, передача данных

Финансирование: Работа авторов из Университета ИТМО выполнена при финансовой поддержке федерального проекта «Передовые инженерные школы» в части исследований ряда динамических характеристик, а также при поддержке Министерства науки и высшего образования Российской Федерации, проект тематики научных исследований № 2019-1442 в части ряда исследований статических характеристик.

Ссылка при цитировании: Ковач Я.Н., Блохин С.А., Бабичев А.В., Бобров М.А., Блохин А.А., Гладышев А.Г., Новиков И.И., Карачинский Л.Я., Воропаев К.О., Егоров А.Ю. Волоконно-оптический передатчик спектрального диапазона 1.55 мкм на основе вертикально-излучающего лазера, изготовленного с применением технологии спекания пластин // Научно-технические ведомости СПбГПУ. Физико-математические науки. 2023. Т. 16. № 1.3. С. 163–169. DOI: https://doi.org/10.18721/ JPM.161.328

Introduction

The demands for the traffic-carrying capacity are constantly growing, which increases the requirements for the data rate of near-IR vertical cavity surface emitting lasers (VCSELs) used in optical interconnects based on multimode fiber [1], but stimulates interest in the search for new optical interconnects based on long-wavelength VCSELs for use in large data centers [2]. The manufacturing of VCSELs based on monolithic InAlGaAsP/InP heterostructures (created in a single epitaxial process) is associated with poor thermal conductivity and low contrast in the refractive indices of ternary and quaternary solutions, which negatively affects both the optical output power of the laser and its high-speed performance [3]. The most promising way for VCSEL manufacturing in the 1.3/1.55 μm spectral range is the hybrid integration of an active region based on InAlGaAs/InP materials either with high-contrast dielectric mirrors based on $CaF_2(AlF_3)/ZnS$ materials [4–6], or with distributed Bragg reflectors (DBR) based on AlGaAs/GaAs materials using wafer-fusion technology (WF-VSCEL) [7–10]. In terms of the active region used, two main approaches can be distinguished: thick InAlGaAs quantum wells [4–6, 10] or thin strained InGaAs quantum wells [8, 9].

In this paper, we present the results of studies of an optical-fiber transmitter based on 1.55 μm WF-VCSEL with strained InGaAs quantum wells used as active region. An evaluation of the maximum bit rate and range of data transmission over single-mode fiber with different lengths has also been carried out.

Device Structure and Fabrication

The main element of studied optical-fiber transmitter (VCSEL-based transmitter) was VCSEL with current injection implemented by *n*-InP intracavity contacts and n^{++}-InAlGaAs/p^{++}-InAlGaAs tunnel junction (TJ). Active area of VCSEL contained seven strained quantum wells InGaAs with InAlGaAs barrier layers. The optical cavity with the total length 3λ confined by top and bottom DBR based on 35 and 22 quarter-wave pairs of AlGaAs/GaAs layers. Current and optical confinements were implemented within the concept of a buried tunnel junction (BTJ). Due to partial planarization of surface relief in TJ layers, single-mode lasing was feasible at large BTJ mesa diameters.

A detailed description of the VCSEL hybrid heterostructure and VCSEL chip manufacturing is presented in [11] and [12]. A single VCSEL chip with 7 µm BTJ mesa diameter was mounted in an HF-case with a SMA-connector and an optical FC/APC connector. The VCSEL was optically coupled into a SMF-28 fiber by conical microlens formed on the fiber end.

Device Characterizations and Discussions

Fig. 1 shows the basic static and spectral characteristics of the VCSEL-based transmitter. The efficiency of optical coupling into a single-mode fiber was about 45 %, which ultimately limited the maximum output optical power to 2.5 mW (Fig. 1, *a*). At the same time the value of threshold current did not exceed 1.4 mA. The studied optical-fiber transmitter showed single-mode lasing with side mode suppression ratio (SMSR) more than 30 dB in the wide range of operating current (Fig. 1, *b*).

The frequency splitting of the fundamental mode is associated with the degeneracy removal of the two orthogonal polarized modes (birefringence) [13], which was caused by transverse anisotropy of the cavity resulted from the asymmetric form of the re-grown BTJ mesa [7] and/or the elasto-optic effect induced by the mechanical strain after the double wafer-fusion [14]. An analysis of frequency splitting mechanisms is beyond the scope of this paper.

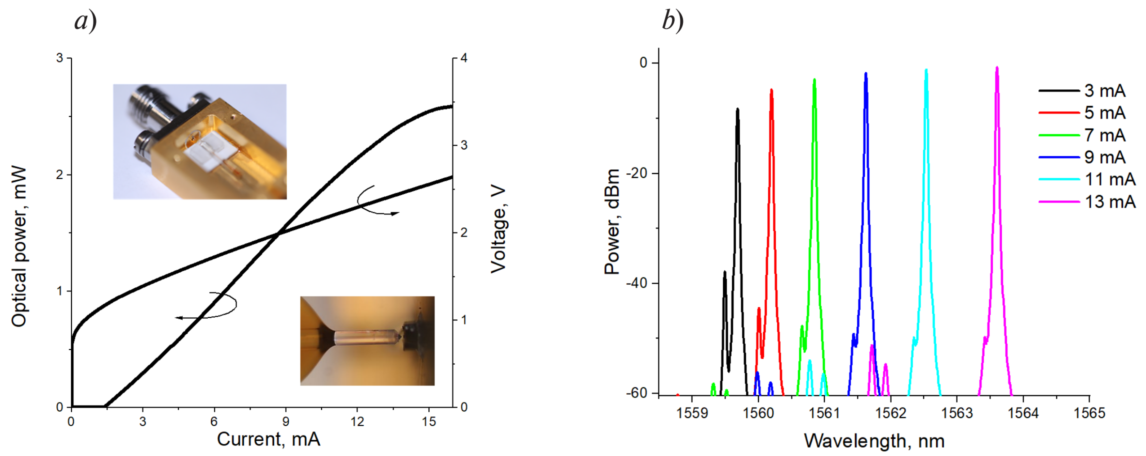

Fig. 1. Light output power and voltage as function of the current (*a*) and the typical optical spectra obtained at 20 °C (*b*)

Fig. 2 shows the results of small-signal modulation analysis of the VCSEL-based transmitter using a Rodhe & Schwarz ZVA 40 network analyzer and a New Focus 1434 photodetector at 25 GHz. Above the threshold current the −3 dB modulation bandwidth gradually increased with modulation current efficiency factor ~3.8 GHz/mA$^{0.5}$ and reached saturation at the values of 11.5-12 GHz under the current over 10 mA. The rate of resonance frequency increment with current above threshold (D-factor) reached 2.7 GHz/mA$^{0.5}$ and showed tendency to saturate at higher injection current. In addition, resonant frequency is below the -3 dB modulation bandwidth in the entire range of operating currents. The K-factor estimated from the dependence of the intrinsic damping factor on the square of the resonant frequency was 0.35 ns at moderate photon densities. The achieved modulation bandwidth of the optical-fiber transmitter was higher in comparison with unmounted VCSEL chip [9], which can be explained by the improvement of the electrical matching between the mounted VCSEL chip and a microwave signal source in the frequency range of 6-10 GHz. The high-speed performance of direct modulated laser is determined by the damping of the relaxation oscillation, the thermal effect and the cut-off frequency of the electrical parasitic [15]. The maximum theoretical bandwidth limited by damping was estimated to be 25 GHz, however the effects of self-heating and gain saturation at large currents enhanced the damping. The maximum theoretical bandwidth limited by the electrical parasitics was more than 20 GHz, while the maximum theoretical bandwidth limited by the thermal effects was about 16 GHz. Thus, the high-speed performance of the VCSEL-based transmitter was limited by a combination of thermal effects with damping of relaxation oscillations.

To evaluate the data transmission capacity under on-off keying modulation the optical-fiber transmitter was modulated by a large non-return-to-zero (NRZ) signal. A Keysight M8195A arbitrary waveform generator was used to form a pseudorandom binary sequence (PRBS) with the length of (2^7-1) bit. Eye diagrams were registered by a Keysight UXR0204A real-time oscilloscope with a Keysight N7004A optical-electrical converter. Fig. 3, *a* shows the measured eye

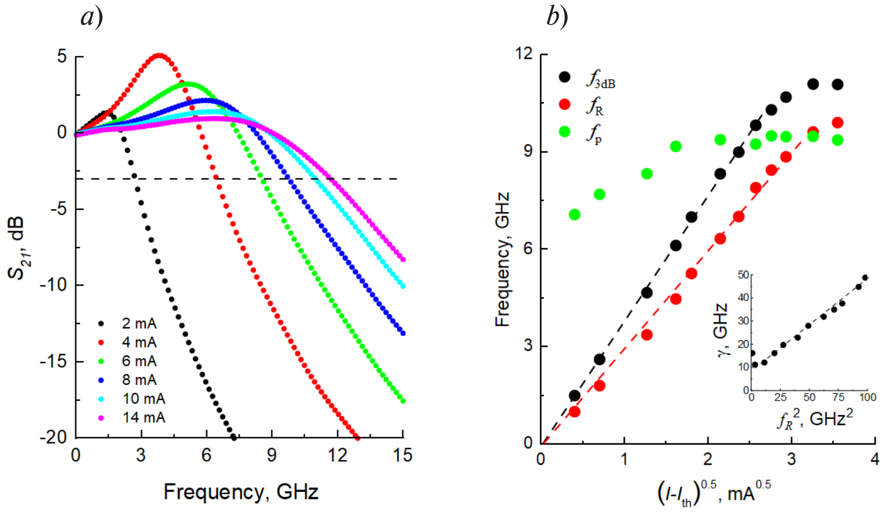

Fig. 2. Measured small signal modulation response S_{21} at the different currents (*a*); parasitic cut-off frequency f_p, resonance frequency f_R and −3dB modulation bandwidth f_{-3dB} as function of the squared root of the current above threshold (*b*). The inset shows the dependence of the intrinsic damping factor γ on the square of the resonant frequency f_R^2. The temperature of measurements was 20 ºC

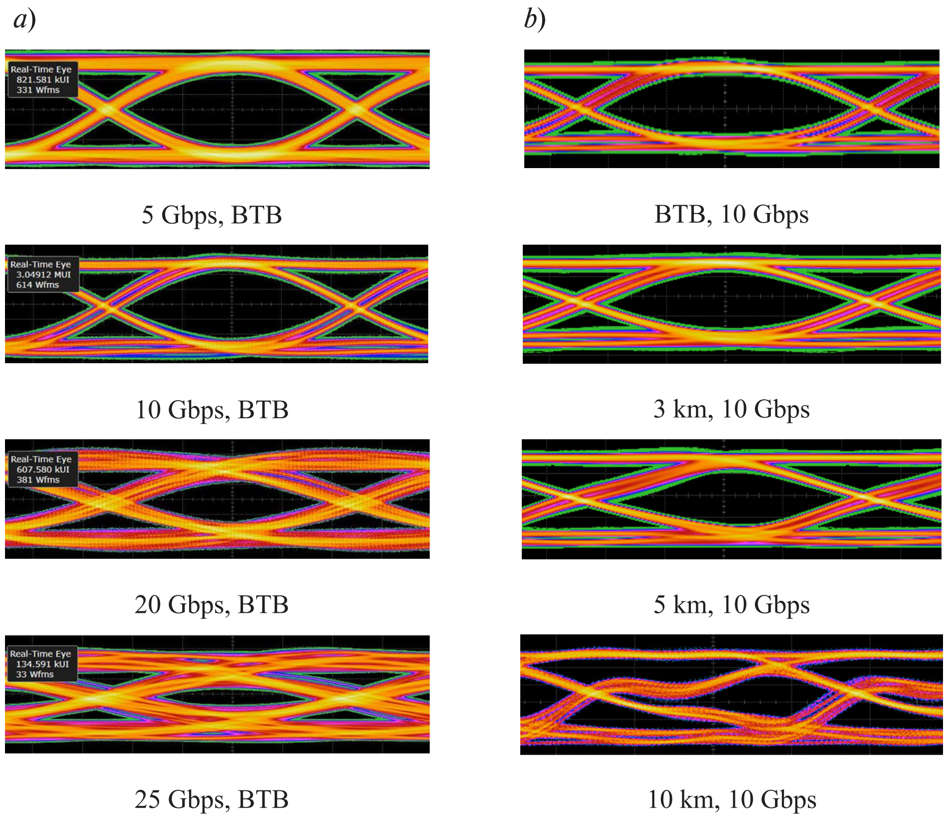

Fig. 3. Optical eye diagrams at different bit rates across a 1 m SMF-28 fiber (*a*); optical eye diagrams at 10 Gbps for different lengths of SMF-28 fiber (*b*). The operating current was 10 mA, the modulating voltage was 0.5 V. The measurement temperature was 20 ºC

diagrams of optical-fiber transmitted at different data rates for short transmission line (back-to-back, BTB). At the bit rates higher than 10 Gbps, enhancement of inter-symbol interference can be seen, which leads to increase in jitter and decrease in eye height, despite the relatively high optical modulation amplitude. It should be mentioned that high rise and fall times (~25 ps) of input electrical signal, which is formed by PRBS-generator, also negatively affect the shape of the decision area (eye width and height). Influence of SMF transmission on the shape of the eye diagrams was also studied at bit rate of 10 Gbps (Fig. 3, *b*). As the fiber length increases, the rise/fall time firstly increases from ~40 to ~100 ps, and the pulse splits within the clock interval into separate groups of lines with different signal rise/fall times (after 7 km SMF transmission).

Fig. 4, *a* shows the optical spectra of the VCSEL-based transmitter at different bit rates of PRBS (2^7-1) NRZ modulation. Compared to CW operation, a decrease in the bit rate leads to the greater red shift of the lasing spectrum, while an increase in the bit rate leads to a significant spectrum broadening (positive chirp). A wider spectrum of the optical signal leads to an increase in the rise and fall edges of the signal due to the chromatic dispersion of the optical fiber, which correlates with the experimental eye diagrams (Fig. 3, *b*).

In order to clarify the influence of individual bit sequences on the lasing spectrum of a fiber-optic transmitter, the spectra were studied under amplitude modulation by rectangular pulses of various durations with a repetition rate of 500 MHz, simulating a sequence of *n* bits "1" at bit rate of 10 Gbit/s. As shown in Fig. 4, *b*, as the pulse duration increases (the sequence of bits "1"), a red shift of the emission spectrum is observed, which is due to fluctuations in the material parameters of the laser cavity and the active region caused by the modulation of the charge carrier density. Therefore, it can be assumed that the faster components of the eye diagram, corresponding to the bit sequence 01010, are blue shifted compared to the slower components of the eye diagram, corresponding to sequences of identical bits. Thus, the combination of positive chirp of optical pulses and positive chromatic dispersion of the SMF-28 fiber leads to an increase in the rise/fall time of the slower components of the eye diagram compared to the faster components, which ultimately leads to distortion of the shape of the eye diagram for a fiber length more than 7 km.

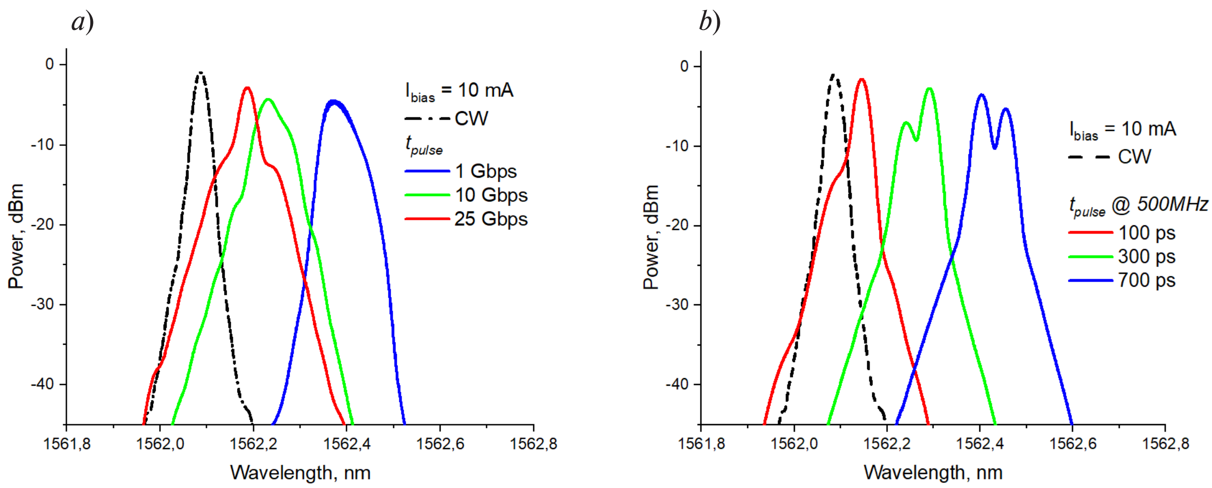

Fig. 4. Optical spectra of the VCSEL-based transmitter modulated at different bit rates (*a*); optical spectra of the VCSEL-based transmitter modulated at 500 MHz frequency with different pulse time (*b*)

Conclusion

The static and dynamic characteristics of a 1.55 µm VCSEL-based transmitter were studied. The device demonstrates single-mode generation with SMSR >30 dB over a wide range of currents, and the maximum optical power at the fiber end exceeds 2.5 mW. According to small-signal modulation experiments the -3 dB modulation bandwidth exceeded 11 GHz. The high-speed performance of the device is limited by thermal effects and damping of relaxation oscillations.

The analysis of the maximum bit rate and fiber length was carried out. The maximum bit rate exceeded 25 Gbps and was limited by the characteristics of the PRBS generator. With an increase of the fiber length, an increase of the rise and fall times was observed, which was caused by the dynamic broadening of the spectrum (chirping). According to the analysis of the emission spectra for various modulations, the slower components were red shifted compared to the fast components. As a result, the chromatic dispersion of the fiber led to increased inter-symbol interference and limited the length of the fiber for data transmission.

REFERENCES

1. **Padullaparthi B.D., Tatum J., Kenichi I.,** VCSEL Industry: Communication and Sensing. John Wiley & Sons, 2021.

2. **Zhang L., Van Kerrebrouck J., Lin R., Pang X., Udalcovs A., Ozolins O., Spiga S., Amann M.-C., Van Steenberge G., Gan L., Tang M., Fu S., Schatz R., Popov S., Liu D., Tong W., Xiao S., Torfs G., Chen J., Yin X.,** Nonlinearity Tolerant High-Speed DMT Transmission With 1.5-μm Single-Mode VCSEL and Multi-Core Fibers for Optical Interconnects. Journal of Lightwave Technology, 37(2), (2019), 380—388.

3. **Park M.-R., Kwon O.-K., Han W.-S., Lee K.-H., Park S.-J., Yoo B.-S.,** All-epitaxial InAlGaAs-InP VCSELs in the 1.3-1.6-/spl mu/m wavelength range for CWDM band applications. IEEE Photonics Technology Letters, 18(16), (2006), 1717—1719.

4. **Muller M., Hofmann W., Grundl T., Horn M., Wolf P., Nagel R. D., Amann M. C.,** 1550-nm high-speed short-cavity VCSELs. IEEE Journal of selected topics in Quantum Electronics, 17(5), (2011), 1158–1166.

5. **Spiga S., Schoke D., Andrejew A., Boehm G., Amann M.-C.,** Effect of Cavity Length, Strain, and Mesa Capacitance on 1.5-μm VCSELs Performance. Journal of Lightwave Technology, 35(15), (2017), 3130—3141.

6. **Spiga S., Soenen W., Andrejew A., Schoke D. M., Yin X., Bauwelinck J., Boehm G., Amann M.-C.,** Single-Mode High-Speed 1.5-μm VCSELs. Journal of Lightwave Technology, 35(4), (2017), 727—733.

7. **Sirbu A., Iakovelv V., Mereuta A., Caliman A., Suruceanu G., Kapon E.,** Wafer-fused heterostructures: application to vertical cavity surface-emitting lasers emitting in the 1310 nm band. Semiconductor Science and Technology, 26(1), (2011), 014016.

8. **Blokhin S.A., Babichev A.V., Gladyshev A.G., Novikov I.I., Blokhin A.A., Bobrov M.A., Maleev N.A., Andryushkin V.V., Denisov D.V., Voropaev K.O., Ustinov V.M., Bougrov V.E., Egorov A.Y., Karachinsky L.Y.,** 20-Gbps 1300-nm range wafer-fused vertical-cavity surface-emitting lasers with InGaAs/InAlGaAs superlattice-based active region. Optical Engineering, 61(09), (2022).

9. **Babichev A.V., Karachinsky L.Y., Novikov I.I., Gladyshev A.G., Blokhin S.A., Mikhailov S., Iakovlev V., Sirbu A., Stepniak G., Chorchos L., Turkiewicz J.P., Voropaev K.O., Ionov A.S., Agustin M., Ledentsov N.N., Egorov A.Y.,** 6-mW Single-Mode High-Speed 1550-nm Wafer-Fused VCSELs for DWDM Application, IEEE Journal of Quantum Electronics, 53 (6) (2017) 1—8.

10. **Ellafi D., Iakovlev V., Sirbu A., Grigore S., Mickovic Z., Caliman A., Mereuta A., Kapon E.,** Effect of Cavity Lifetime Variation on the Static and Dynamic Properties of 1.3-μm Wafer-Fused VCSELs. IEEE Journal of Selected Topics in Quantum Electronics, 21(6), (2015), 414—422.

11. **Blokhin S.A., Bobrov M.A., Blokhin A.A., Kuzmenkov A.G., Maleev N.A., Ustinov V.M., Kolodeznyi E.S., Rochas S.S., Babichev A.V., Novikov I.I., Gladyshev A.G., Karachinsky L.Y., Denisov D.V., Voropaev K.O., Ionov A.S., Egorov A.Y.,** Analysis of the Internal Optical Losses of the Vertical-Cavity Surface-Emitting Laser of the Spectral Range of 1.55 μm Formed by a Plate Sintering Technique, Optics and Spectroscopy, 127(1), (2019), 140—144.

12. **Voropaev K.O., Seleznev B.I., Prokhorov A.Y., Ionov A.S., Blokhin S.A.,** The fabrication technology of VCSELs emitting in the 1.55 μm waveband, Journal of Physics: Conference Series, 1658(1), (2020), 012069.

13. **Volet N., Iakovlev V., Sirbu A., Caliman A., Suruceanu G., Mereuta A., Kapon E.,** Polarization mode structure in long-wavelength wafer-fused vertical-cavity surface-emitting lasers. In Semiconductor Lasers and Laser Dynamics V, 8432, (2012), 76–86.

14. **Yu J.L., Chen Y.H., Jiang C.Y., Ye X.L., Zhang H.Y.,** Detecting and tuning anisotropic mode splitting induced by birefringence in an InGaAs/GaAs/AlGaAs vertical-cavity surface-emitting laser. Journal of Applied Physics, 111(4), (2012), 043109.

15. **Blokhin S.A., Maleev N.A., Bobrov M.A., Kuzmenkov A.G., Sakharov A.V., Ustinov V.M.,** High-speed semiconductor vertical-cavity surface-emitting lasers for optical data-transmission systems. Technical Physics Letters, 44(1), (2018), 1–16.

THE AUTHORS

KOVACH Yakov N.
yakovachyakov@gmail.com
ORCID: 0000-0003-4858-4968

BLOKHIN Sergey A.
blokh@mail.ioffe.ru
ORCID: 0000-0002-5962-5529

BABICHEV Andrey V.
andrey.babichev@connector-optics.com
ORCID: 0000-0002-3463-4744

BOBROV Mikhail A.
bobrov.mikh@gmail.com
ORCID: 0000-0001-7271-5644

BLOKHIN Alexey A.
bloalex91@yandex.ru
ORCID: 0000-0002-3449-8711

GLADYSHEV Andrey G.
andrey.gladyshev@connector-optics.com
ORCID: 0000-0002-9448-2471

NOVIKOV Innokenty I.
innokenty.novikov@itmo.ru
ORCID: 0000-0003-1983-0242

KARACHINSKY Leonid Ya.
leonid.karachinsky@connector-optics.com
ORCID: 0000-0002-5634-8183

VOROPAEV Kirill O.
kirill.voropaev@novsu.ru
ORCID: 0000-0002-6159-8902

EGOROV Anton Yu.
anton.egorov@connector-optics.com
ORCID: 0000-0002-0789-4241

Received 14.12.2022. Approved after reviewing 25.01.2023. Accepted 25.01.2023.